Is $U_3Ni_3Sn_4$ best described as near a quantum critical point?

C. H. Booth,[1] L. Shlyk,[2] K. Nenkov,[2,3] J. G. Huber,[4] and L. E. De Long[4]

[1] *Chemical Sciences Division, Lawrence Berkeley National Laboratory, Berkeley, California 94720, USA*

[2] *IFW, Institute for Solid State and Materials Research, POB 270016, 01171 Dresden, Germany*

[3] *International Laboratory of High Magnetic Fields and Low Temperatures, Gajowicka 95, 53-529, Wroclaw, Poland*

[4] *Department of Physics and Astronomy, University of Kentucky, Lexington, KY 40506-0055, USA*

(Dated: Draft: July 2, 2002)

Abstract

Transport and thermodynamic measurements on $U_3Ni_3Sn_4$ display many of the properties consistent with a system near a zero-temperature magnetic/nonmagnetic phase boundary. The role of any possible structural or magnetic disorder, however, remains unclear. Measurements of the x-ray absorption fine structure (XAFS) on $U_3Ni_3Sn_4$ at the U $L_{\rm III}$, Ni K and Sn K edges are reported. Temperature dependent measurements were performed on polycrystal samples with various stoichiometries. Measurements at 20 K on single crystals are also reported. No evidence of lattice disorder is observed, placing upper limits on the amount of possible lattice disorder in these materials. These measurements rule out models with a relatively strong sensitiviety to disorder, such as most variants of the Kondo disorder model, but do not rule out a more subtle dependence of NFL behavior on lattice disorder. However, we also report measurements of the specific heat in applied magnetic fields and of the sample magnetization scaling with temperature and applied field that indicate the essential physics is not that of single-impurity interactions and that the system is very close to a zero-temperature magnetic phase transition. Taken together with previous data, this study provides yet more evidence that the physics of the $U_3Ni_3Sn_4$ system is best described within the antiferromagnetic quantum critical point framework.

PACS numbers: 72.15.Qm, 61.10.Ht, 71.23.-k, 71.27.+a

I. INTRODUCTION

$U_3Ni_3Sn_4$ displays characteristic non-Fermi liquid behavior (NFL). For instance, the low-temperature magnetic susceptibility χ diverges as $T^{-0.3}$, the Sommerfeld coefficient for the electronic term in the specific heat $\gamma = C_{el}/T$ diverges as $-T^{0.5}$, and the resistivity changes as $T^{1.79}$. Such behavior is at odds with the Fermi liquid (FL) description ($\chi \sim C_{el}/T \sim$ const., $\Delta\rho \sim T^2$) of Landau[1] that is thought to apply to this system. This article attempts to differentiate between the applicability of various possible theoretical models describing non-Fermi liquid behavior in this system by searching for the presence of local lattice disorder, how the FL/NFL crossover temperature is affected by applied magnetic fields, and how the sample magnetization scales with applied field and temperature.

The various theoretical models describing NFL behavior fall into a few general classes, including close proximity to a zero-temperature phase transition, competition between interactions such as Ruderman-Kittel-Kasuya-Yosida (RKKY) and Kondo effects, single-impurity verses non-single-impurity models, and those that include magnetic-interaction disorder. For instance, non-Fermi liquid behavior in the high-temperature superconductors and in some of the heavy fermion systems has been postulated to be due to the proximity of these systems to a magnetic/nonmagnetic zero temperature phase transition.[2] We will refer to such models as anti- or ferromagnetic quantum critical point (AF-QCP or (FM-QCP) models. Indeed, most f-electron intermetallic NFL materials have been demonstrated to be near such a point, manifest by driving the system into a magnetic phase with applied magnetic fields, pressure or chemical substitution (chemical pressure).[3] Millis[4] and others[5–8] have developed the theory of critical fluctuations at temperatures above such a magnetic/non-magnetic quantum critical point, building off earlier work by Hertz.[9] The presence of a nearby magnetic phase is not necessary to obtain an NFL state, however. For instance, a multichannel Kondo model[10] also gives non-Fermi liquid behavior. In addition, even though these theories have unique magnetic interaction strengths between the f and the conducting electrons, all of the first materials identified that display NFL properties at ambient pressure also contain some form of lattice disorder, usually in the form of chemical substitution. This raises the possiblity that lattice disorder plays an important role. In fact, a broad distribution of effective moments has been observed in several systems (for instance, $CeRhRuSi_2$[11] and $UPdCu_4$[12]). These observations prompted researchers to consider the role of magnetic in-

teraction disorder as a microscopic origin for non-Fermi liquid effects. One simple theory only utilizes the Fermi liquid concept of a distribution of Kondo interactions, and is known as the Kondo disorder model (KDM).[12,13] Other models that consider disorder in the vicinity of a zero-temperature fixed point are known as Griffiths' phase models (note that the KDM is also a Griffiths' phase model, but is not generally classified as such since the domain size is not a necessary component). These include the Griffiths'-McCoy singularities that occur in a disordered Kondo system but whose properties are mostly derived from rare clusters where antiferromagnetic RKKY interactions persist.[14,15] Another possible origin of a Griffiths' phase occurs when disorder-induced Anderson localization occurs in the vicinity of a metal-insulator transition.[16] To clarify the discussion, we will refer to the former model as the antiferromagnetic Griffiths' phase, or AF-GP, and to the latter model as the metal-insulator transition Griffiths' phase, or MIT-GP.

Although many NFL materials exist that have some intrinsic disorder, apparently supporting the disorder models of NFL behavior, a growing number of new materials have been identified that appear to be stoichiometric, structurally well-ordered NFL systems at ambient pressure. Some examples include $YbRh_2Si_2$,[17] $CeNi_2Ge_2$,[18] $CeCoIn_5$[19] and $U_3Ni_3Sn_4$.[20] Although some of the physical properties of these systems agree with those predicted by the QCP model proposed by Millis, none of these materials display properties that universally agree with it. In addition, it is difficult to uniquely differentiate measured behavior between the "pure" QCP models and the Griffiths' phase models, especially since the Griffiths' models have critical exponents that depend on the degree of disorder that are, at this time, impossible to relate to real measures of disorder.[21] Such is the case for $U_3Ni_3Sn_4$.

Careful consideration of the disorder-based and QCP models involves comparisons both of electronic and magnetic properties to theory and thorough characterization of the degree of structural and magnetic order of the samples. The $U_3Ni_3Sn_4$ situation is complicated by the fact that $U_3Ni_3Sn_4$ has been shown to have a Fermi liquid ground state below about 0.4-0.5 K, with NFL behavior occuring above this crossover region.[22] Regardless, in the NFL region, the electrical resistivity goes as $\Delta\rho = \rho(T) - \rho_0 \sim T^{1.79}$,[20] roughly consistent with the AF-QCP result of $\Delta\rho \sim T^{1.5}$,especially if one considers the possibility of Fermi liquid and non-Fermi liquid regions. The magnetic susceptibility χ diverges as $T^{-0.3}$, at odds with the predictions of the AF-QCP result of $T^{1.5}$, potentially for similar reasons as the resistivity. The electronic part of the specific heat diverges consistently with the AF-QCP result of

$C_{el}/T \sim -T^{0.5}$. These results can all be self-consistently explained with a Griffiths-McCoy phase[14,15] with a critical exponent of $\lambda = 0.7$, producing only marginally worse fits to the data.[22] These data are also qualitatively consistent with the two-channel Kondo model[23–26], although this model then requires a very high spin-fluctuation energy.[20] Comparisons to the KDM are not favorable for this material, since the KDM predicts logarithmic divergences of the magnetic susceptibility and the specific heat and a linear temperature dependence of the electrical resistivity, all of which are clearly at odds with the experimental data. In addition, measurements at applied pressures up 1.8 GPa[27] indicate that the FL ground state extends to higher temperatures with increasing pressure. A scaling analysis of the FL/NFL crossover temperature as a function of applied pressure strongly implying a negative-pressure magnetic QCP, which has been estimated at -0.04 ± 0.04 GPa.

Although the measured properties of $U_3Ni_3Sn_4$ do not easily differentiate between the various NFL models (except for the KDM), there is little evidence to suggest that any disorder exists in this system, apparently not supporting the Griffiths' phase models. In particular, single crystals of the material form, and x-ray diffraction studies of these crystals show the material to be consistent with the nominal stoichiometry. Moreover, the residual resistivity is reasonably low (7 $\mu\Omega$cm[20]). In spite of the evidence for structural order, some forms of lattice disorder can be difficult to detect using standard diffraction techniques. For instance, if disorder occurs in a non-periodic fashion, such as in glassy regions or very small domains, only a local structural probe such as x-ray absorption fine-structure (XAFS) or pair-distribution function (PDF) analysis of powder diffraction data will be sensitive to it. In addition, no temperature dependent structural studies have been performed, and disorder in the displacement parameters (Debye-Waller factors) can often be misinterpreted as due to large vibrational amplitudes in such cases. Therefore, to continue to test the degree of structural order in $U_3Ni_3Sn_4$, we report below structural measurements using XAFS spectroscopy. Although the structure of $U_3Ni_3Sn_4$ limits the accuracy of the estimated maximal disorder levels as detailed below, our measurements are consistent with no detectable disorder within experimental error, on both single crystals and polycrystals, from temperature dependence and from all three absorption edges.

As implied above, merely having the lattice be (measurably) well ordered may not rule out magnetic interaction disorder. Since the Griffiths' phase models only require "rare" clusters of competing interactions to form, one can only place upper limits on the possible sizes

of such clusters experimentally. In addition, some heretofore more subtle Kondo disorder mechanism may still be applicable (for instance, if large fluctuations in the conduction density of states accompanies fluctuations in the hybridization strength in the presence of lattice disorder[28]). Another dividing line between these theories is the presence of a low-lying magnetic phase. To further test the applicability of these theories, one can infer the presence of a low-lying AF phase transition by looking at changes in the FL/NFL crossover temperature with applied field. Also, one can discriminate against simple single-impurity physics as the root of the NFL behavior by measuring how the sample magnetization scales with temperature and applied field. If the value of the scaling exponent is larger than unity, one can definitively rule out the single impurity theories, such as the KDM (and any more subtle variants) and the multichannel Kondo models. Single-impurity scaling would also rule out the MIT-GP model as it is currently posed. However, once spin-spin interactions are included, the model may no longer follow such scaling.

The rest of this paper is organized as follows. The XAFS measurements are described in Sec. II, including a description of the sample preparation and the technique. Sec. III relates the results from the measurements of specific heat and magnetization as a function of temperature and applied field. These results are discussed in relation to the various NFL theories in Sec. IV, and the final conclusions are summarized in Sec. V.

II. XAFS MEASUREMENTS

A. Background

$U_3Ni_3Sn_4$ crystallizes into a *bcc* structure, in the $I\bar{4}3d$ space group with the lattice parameter 9.3524 Å and an x value of 0.082, which describes the Sn displacements (Fig. 1).[20] Crystallographically, the structure is fairly simple, with a single site for each atomic species. The local environments are quite a bit more complicated, although the nearest-neighbor shells are fairly well separated. For instance, U has 4 nearest neighbor Ni's at 2.86 Å, followed by 8 Sn neighbors at 3.24 Å. Ni has 4 Sn neighbors at 2.61 Å and 4 U neighbors at 2.86 Å. Sn has 3 Ni neighbors at 2.61 Å, followed by 6 U neighbors at 3.24 and 3 Sn neighbors at 3.50 Å. (Fig. 2).

B. Experimental

Samples include three polycrystalline samples with nominal stoichiometries $U_{3.0}Ni_{3.0}Sn_{4.0}$, $U_{2.9}Ni_{3.0}Sn_{3.9}$, and $U_{3.0}Ni_{3.1}Sn_{3.9}$. Two single crystal samples were also measured with nominal stoichiometries of $U_{3.0}Ni_{3.0}Sn_{4.0}$ and $U_{2.9}Ni_{3.0}Sn_{3.9}$, and are the same as those reported in Ref. 20. All XAFS data were collected on beam lines 4-1 and 4-3 at the Stanford Synchrotron Radiation Laboratory (SSRL) using half-tuned Si(220) double monochromator crystals. Samples were placed into a LHe flow cryostat. Polycrystal samples were ground into a fine powder under actetone, passed through a 40 μm sieve and brushed onto scotch tape, with stacked layers corresponding to $\Delta\mu t \approx 1$. Data for the polycrystals were collected at various temperature between 20 K and 300 K at the U $L_{\rm III}$, and Sn K edges in transmission mode, and at the Ni K edge in fluorescence mode using a 4-pixel Ge detector.[29]. Single crystal data were collected at 20 K at the U $L_{\rm III}$ and the Sn and Ni K edges in fluorescence mode. Several scans were obtained for each sample at each edge and temperature, and were fit separately to cross check the error estimates. Dead-time and self-absorption[30] corrections were applied to the fluorescence data. Data were reduced and fit in r-space using the RSXAP package.[31–33] In particular, the XAFS function $\chi(k)$ is defined as $\mu(k)/\mu_E(k) - 1$, where $\mu(k)$ is the absorption coefficient as a function of the wave vector k of the photoelectron, and $\mu_E(k)$ is the so-called "embedded atom" background absorption that is proportional to the number of generated photoelectrons. The wave vector is defined as $k = \sqrt{\frac{2m_e}{\hbar^2}(E - E_0)}$, and the photoelectron threshold energy is defined arbitrarily as the energy at the half-height of the edge, and is allowed to vary in subsequent fits. Examples of the $k\chi(k)$ data are shown in Fig. 3 for the polycrystal samples. Data on single crystals is similar, both in quality and quantity.

Each data set was fit with a single value of the XAFS amplitude reduction factor S_0^2, assuming full nominal site occupancies. This assumption places the effect of vacancies on the Debye-Waller parameters. All scattering paths share a single value of E_0. In the case where multiple temperatures were collected, an average S_0^2 and E_0 were obtained and then held fixed for all temperatures for a given edge. Data on the single crystals were fit with different S_0^2 and E_0 than the polycrystal data, although no major differences were observed. Reported error estimates use the larger of either a Monte Carlo estimate of the 1-standard deviation displacements (essentially equivalent to a covariance matrix without

having to assume that the statistical-χ^2 is quadratic near its minimum), or the distribution of parameters obtained by fitting the individual scans at each temperature. Reported errors are generally consistent with those obtained from standard compounds, typically 0.005 Å in pair distance and 10-20% in σ^2 for near neighbors, with the error roughly doubling after about 3 Å.[32]

C. Results

Fig.s 4 and 5 show the Fourier transforms (FT) of $k^3\chi(k)$. Peaks in the FT's correspond to pairs in the local structure, however, it must be noted that constructive/destructive interference can occur (the functions are complex), the scattering profiles are not Gaussian, and phase shifts occur that place the peaks at distance in the FT's that are shorter than in the structure by an amount related to the species of absorber and backscatterer. Transmission data were collected out to a $k_{\max} = 15$ Å, and fluorescence data were collected out to a $k_{\max} = 13$ Å. Fig. 5 shows a proper comparison between the single and polycrystal data for the $U_{3.0}Ni_{3.0}Sn_{4.0}$ samples with the same transform ranges.

There are visible differences between the various data sets for a given edge. In particular, the polycrystal $U_{3.0}Ni_{3.1}Sn_{3.9}$ Ni and Sn edge data consistently show a reduced amplitude compared to $U_{3.0}Ni_{3.0}Sn_{4.0}$ at all temperatures, consistent with some disorder or the presence of an amorphous phase containing those elements. Although these differences are above the signal to noise, it is not possible to discern the exact cause of the differences from the fit results listed below. Differences between the polycrystal and the single crystal data (Fig. 5) are similar in magnitude, but complications with analyzing single crystal data, such as dead-time and self-absorption corrections, are very likely the cause.

The basic procedure used here for searching for lattice disorder is to carry out fits assuming the nominal structure, then examine certain parameters for signs of disorder. In the fits, each distinct scattering shell in the nominal structure out to about 4.7 Å is used at each edge. The scattering amplitudes are all set to NS_0^2, where N is the nominal number of neighbors in a given shell for the stoichiometric compound, and S_0^2 is the XAFS amplitude scale (reduction) factor. Each scattering pair is allowed to vary its pair distance (bond length), R and its pair-distance distribution width , σ^2 (the Debye-Waller factor). Applying all these constraints drastically reduces the number of fit parameters, but assigns all the sources of

lattice disorder into either the measured bond lengths of the Debye-Waller factors.

Fit results to the data from the polycrystal samples are shown in Table I, and are compared to results inferred from diffraction measurements. Fit quality is very high; examples of the fit quality are shown in Fig. 6. Although all the polycrystal data were collected as a function of temperature, we only show the fit results for the coldest measured temperature. No significant changes in the fit parameters occur with temperature, except that the Debye-Waller factors increase in a manner consistent with the correlated-Debye model[34] plus a temperature-independent offset $\sigma^2_{\rm static}$. Such offsets can be used as indicators for non-thermal disorder (a prime example occurs in the colossal magnetoresistance manganese perovskites[35]), but we see no evidence for $\sigma^2_{\rm static}$ values inconsistent with zero disorder. Results for the correlated-Debye temperature $\Theta_{\rm cD}$ and $\sigma^2_{\rm static}$ are shown in Table I. Note that the preponderence of small, unphysically negative measurements of $\sigma^2_{\rm static}$ are likely due to small underestimates of S_0^2.

Fit results to the single crystal data were found to be the same as results from the polycrystal data, within the error estimates, and so are not reported here. No evidence for lattice disorder is observed, as exemplified by the consistently low values of the nearest-neighbor σ^2's for the low temperature fits.

Finally, the possiblity of site interchange, or site/anti-site disorder was also considered. This possibility is very remote, however, given the big differences in the radii of the atoms involved, except for Sn/U interchange (covalent radii are 1.42 Å, 1.15 Å, and 1.41 Å for U, Ni and Sn, respectively). Unfortunately, fitting the Sn and U XAFS data including some U/Sn interchange gives only a broad result: $s = 9 \pm 10\%$, where s is the percentage of Sn sitting on U ($12a$) sites. Fits including U/Ni and Sn/Ni site interchange produced nearly the same results. The principle difficuly in using XAFS to make this measurement is that the local nearest-neighbor environments each have pair distances near $\sim$2.7 Å and then near 3.2 Å, that is, no new peaks would appear in these spectra if site interchange occurs. This situation is in contrast to that in the $UPdCu_4$ system.[36] In any case, the single crystal diffraction results should not have produced such high quality fits[20] if much more than 5% of such interchange occurs.

III. FIELD-DEPENDENT MEASUREMENTS

The specific heat of a $U_3Ni_3Sn_4$ single crystal was measured between 1.8 and 30 K in applied magnetic fields up to 8 T using a Quantum Design PPMS. The specific heat data is shown in Fig. 7, plotted as C_{el}/T versus $T^{0.5}$. Here we have already subtracted the hyperfine and lattice contribution according to the specific heat data of $U_3Ni_3Sn_4$ reported previously.[22] In zero applied magnetic field the data follow the $C_{el}/T \propto T^{0.5}$ behavior below 6 K indicative of non-Fermi liquid regime. Magnetic fields progressively depress the specific heat so that C_{el}/T shows a deviation from square root behavior at lower temperatures. It is expected that C_{el}/T starts to be constant at temperatures lower than 1.8 K, reaching the Fermi-liquid regime. These results strongly imply that applied fields take the system further away from an antiferromagnetic critical point.

The magnetization was measured with a SQUID magnetometer at temperatures down to 1.8 K and in fields up to 7 T. These data are shown in Fig. 8. The magnetization data are plotted to demonstrate that they can be scaled according to the phenomenological theory of non-Fermi-liquid heavy-fermion alloys[37]:

$$M = \frac{H}{T^{\gamma}} \mathrm{F}\left(\frac{H}{T^{\beta+\gamma}}\right),$$

where $\beta + \gamma = 1.3$. The magnetic field therefore has a scaling dimension greater than 1, which is inconsistent with the single impurity models.

IV. DISCUSSION

Deviations from the nominal structure in the fit results can occur in a number of ways. First, the measured S_0^2 amplitude reduction factors should be in a range that has been experimentally measured before. This is, indeed, the case.[32,36] Second, we measure the temperature dependence of the Debye-Waller factors, compare them to a correlated-Debye model, and look for large offsets that can be interpreted as static (i.e. non-thermal) disorder or distortions. In all cases, we see no abnormally large offsets. Third, the measured pair distances should be reasonably close to those measured by diffraction, which is consistent with our measurements (Table I). Fourth, we have considered various site-interchange possiblities, such as U sitting on the (nominally) Sn (16c) site. Although these fits are not particularly sensistive to such interchanges, our measurements are consistent with no site

interchange. Finally, the results from the single crystal and the polycrystal samples are virtually identical. Together with the single crystal diffraction data, we must conclude that the $U_3Ni_3Sn_4$ system is structurally well ordered, and is much more ordered than, say, the $UPdCu_4$ system.[35,38] Although such crystalline order does not rule out some other source of magnetic- interaction disorder that might be consistent with a Kondo disorder model or a Griffiths phase model, it certainly rules out the most likely source. In addition, although these structural studies cannot rule out the presence of small amounts of disorder, previous work within a Kondo disorder model has shown that significantly more disorder would have to be present for that model to work.[38]

There are other requirements for an AF-QCP theory, of course. For one, the system must be very near a magnetic/non-magnetic instability. Measurements under applied pressure indicate this instability may exist at a small negative pressure, based on a scaling of the resistivity behavior. We thus expect that if the magnetic phase is antiferromagnetic, an applied magnetic field will also take one more toward a Fermi liquid regime. The data presented in Fig. 7 indicate this system behaves exactly as one expects if the system is near a magnetic/non-magnetic instability, and are therefore consistent with those that include antiferromagnetism as a competing interaction.

Finally, the observation of a magnetization scaling exponent greater than unity rules out the single-impurity-based theories (Fig. 8). These include the KDM, multichannel Kondo, and the MIT-GP theories. The MIT-GP theory, however, could include spin-spin interactions that were not included in the original calculations for simplicity, so it remains to be seen how the magnetization will scale when such interactions are included.[39]

Taking all these results together, we have ruled out the KDM and multichannel Kondo theories, and partially ruled out the MIT-GP theory. The AF-QCP and the AF-GP theories are still consistent with most of the data, however, there is no indication of any lattice disorder in these materials, and so we must conclude that, currently, the best description of all the available data is that of an antiferromagnetic quantum critical point.

V. CONCLUSION

In summary, we have measured the local structure around the constituent atoms in $U_3Ni_3Sn_4$ single and poly crystals as a function of temperature and stoichiometry. These data

follow typical Debye model dependences in the measured pair-distance distribution widths with no (non-thermal) offsets, as well as agreeing well with the average structure given by previous single crystal diffraction studies.[20] In combination with these previous diffraction studies and the relatively low residual resistivity, all the structural evidence indicates that this system is structurally well ordered. We also report specific heat data that show a clear recovery of Fermi liquid behavior under modest applied magnetic fields, indicating a probable "negative field" quantum critical point, consistent with work under applied pressure that indicates a negative-pressure QCP. Finally, we show that the sample magnetization scales with temperature and applied field with critical exponents that are inconsistent with single-ion (Kondo) physics as the principle NFL mechanism. Taken together, these and all other published results are inconsistent with any disorder-based models or other single-ion based models, yet remain consistent with a system near a very low temperature, antiferromagnetic magnetic instability, that is, an antiferromagnetic quantum critical point.

Acknowledgments

We thank E. D. Bauer, A. J. Millis, E. Miranda, A. H. Castro Neto and D. L. Cox for many useful discussions. This work was partially supported by the Director, Office of Science, Office of Basic Energy Sciences (OBES), Chemical Sciences, Geosciences and Biosciences Division, U.S. Department of Energy (DOE) under Contract No. AC03-76SF00098. XAFS data were collected at the Stanford Synchrotron Radiation Laboratory, which is operated by the DOE/OBES.

---

[1] L. D. Landau, Sov. Phys. JETP **3**, 920 (1957).

[2] See, for example, articles in *Proceedings of the Conference on Non-Fermi Liquid Behavior in Metals*, Santa Barbara, California, 1996, edited by P. Coleman, M. B. Maple, and A. J. Millis, J. Phys.: Condens. Matter **8**, 9675 (1996).

[3] G. R. Stewart, Rev. Mod. Phys. **73**, 797 (2001).

[4] A. J. Millis, Phys. Rev. B **48**, 7183 (1993).

[5] L. B. Ioffe and A. J. Millis, Phys. Rev. B **51**, 16151 (1995).

[6] T. Moriya and T. Takimoto, J. Phys. Soc. Jpn. **64**, 960 (1995).

[7] G. G. Lonzarich, in *The Electron*, edited by M. Springford (Cambridge University Press, New York, 1997), chap. 6.

[8] P. Coleman, Physica B **259-261**, 353 (1999).

[9] J. A. Hertz, Phys. Rev. B **14**, 1165 (1976).

[10] P. Nozières and A. Blandin, J. Phys. (France) **41**, 193 (1980).

[11] T. Graf, J. D. Thompson, M. F. Hundley, R. Movshovich, Z. Fisk, D. Mandrus, R. A. Fisher, and N. E. Phillips, Phys. Rev. Lett. **78**, 3769 (1997).

[12] O. O. Bernal, D. E. MacLaughlin, H. G. Lukefahr, and B. Andraka, Phys. Rev. Lett. **75**, 2023 (1995).

[13] E. Miranda, V. Dobrosavlijević, and G. Kotliar, J. Phys. Condens. Matter **8**, 9871 (1996).

[14] A. H. Castro Neto, G. Castilla, and B. A. Jones, Phys. Rev. Lett. **81**, 3531 (1998).

[15] A. H. Castro Neto and B. A. Jones, Phys. Rev. B **62**, 14975 (2000).

[16] E. Miranda and V. Dobrosavlijević, Phys. Rev. Lett. **86**, 264 (2001).

[17] O. Trovarelli, C. Geibel, S. Mederle, C. Langhammer, F. M. Grosche, P. Gegenwart, M. Lang, G. Sparn, and F. Steglich, Phys. Rev. Lett. **85**, 626 (2000).

[18] F. M. Grosche, P. Agarwal, S. R. Julian, N. J. Wilson, R. K. W. Haselwimmer, S. J. S. Lister, N. D. Mathur, F. V. Carter, S. S. Saxena, and G. G. Lonzarich, J. Phys. Cond. Matt. **12**, L533 (2000).

[19] C. Petrovic, P. G. Pagliuso, M. F. Hundley, J. L. Sarrao, J. D. Thompson, and Z. Fisk, J. Phys.:Condens. Matter **13**, L337 (2001).

[20] L. Shlyk, J. C. Waerenborough, P. Estrela, L. E. DeLong, A. de Visser, and M. Almeida, J. Phys.: Condens. Matter **11**, 3525 (1999), a displacement parameter x=0.082 was obtained, but not reported, in this study.

[21] A. H. Castro Neto (2002), private communication.

[22] L. Shlyk, P. Estela, J. C. Waerenborough, L. E. DeLong, A. de Visser, D. P. Rojas, F. Gandra, and M. Almeida, Physica B **292**, 89 (2000).

[23] D. L. Cox, Phys. Rev. Lett. **59**, 1240 (1987).

[24] D. L. Cox and A. Zawadowski, Adv. Phys. **47**, 599 (1998).

[25] M. Jarrell, H. Pang, D. L. Cox, and K. H. Luk, Phys. Rev. Lett. **77**, 1612 (1996).

[26] M. Jarrell, H. Pang, D. L. Cox, and K. H. Luk, Phys. Rev. Lett. **78**, 1996 (1997).

[27] P. Estrela, A. de Visser, F. R. de Boer, T. Naka, and L. Shlyk, Phys. Rev. B **63**, 212409 (2001).

[28] D. L. Cox (2002), private communication.

[29] J. Bucher, P. G. Allen, N. M. Edelstein, D. K. Shuh, N. W. Madden, C. Cork, P. Luke, D. Pehl, and D. Malone, Rev. Sci. Instrum. **67** (1996).

[30] C. H. Booth, Ph.D. thesis, Univ. of California, Santa Cruz (1996).

[31] T. M. Hayes and J. B. Boyce, in *Solid State Physics*, edited by H. Ehrenreich, F. Seitz, and D. Turnbull (Academic, New York, 1982), vol. 37, p. 173.

[32] G. G. Li, F. Bridges, and C. H. Booth, Phys. Rev. B **52**, 6332 (1995).

[33] See http://lise.lbl.gov/RSXAP/.

[34] E. D. Crozier, J. J. Rehr, and R. Ingalls, in *X-Ray Absorption: Principles, Applications, Techniques of EXAFS, SEXAFS, XANES*, edited by D. Konigsberger and R. Prins (Wiley, New York, 1988), p. 373.

[35] C. H. Booth, F. Bridges, G. H. Kwei, J. M. Lawrence, A. L. Cornelius, and J. J. Neumeier, Phys. Rev. Lett. **80**, 853 (1998).

[36] C. H. Booth, F. Bridges, G. H. Kwei, J. M. Lawrence, A. L. Cornelius, and J. J. Neumeier, Phys. Rev. B **57**, 10440 (1998).

[37] A. M. Tsvelik and M. Reizer, Phys. Rev. B **48**, 9887 (1993).

[38] E. D. Bauer, C. H. Booth, G. H. Kwei, R. Chau, and M. B. Maple (2001), submitted to Phys. Rev. B, http://lise.lbl.gov/chbooth/papers/UCPx.pdf.

[39] E. Miranda (2002), private communication.

Figures

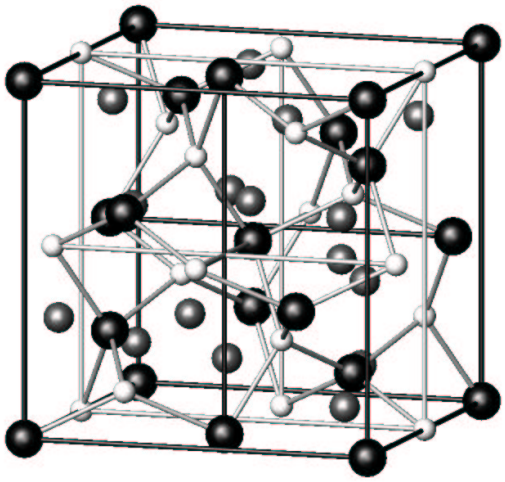

FIG. 1: Crystal structure of $U_3Ni_3Sn_4$. Black balls represent uranium, gray tin and white nickel. The materials is *bcc* with space group $I\bar{4}3d$ and a=9.3524 Å.

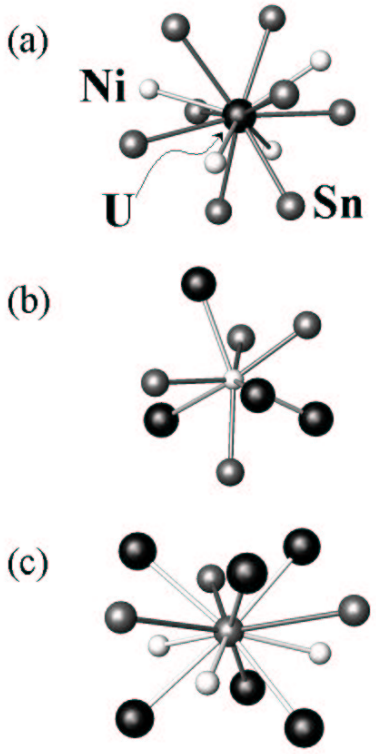

FIG. 2: Local crystal structure from the (a) uranium, (b) nickel, and (c) tin sites. See Sec. II A for details.

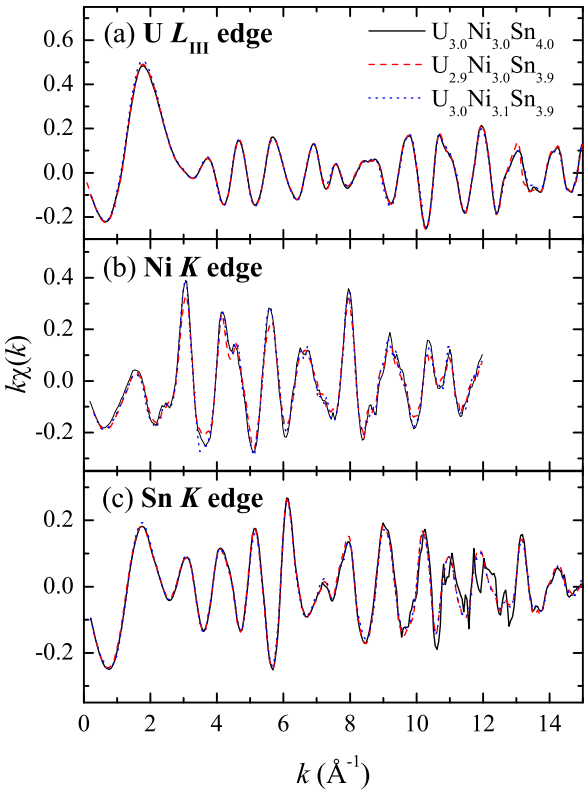

FIG. 3: XAFS data for the three polycrystal samples. Single crystal data is quantitatively similar. Data from the various samples is very similar, and so is difficult to differentiate in the plot.

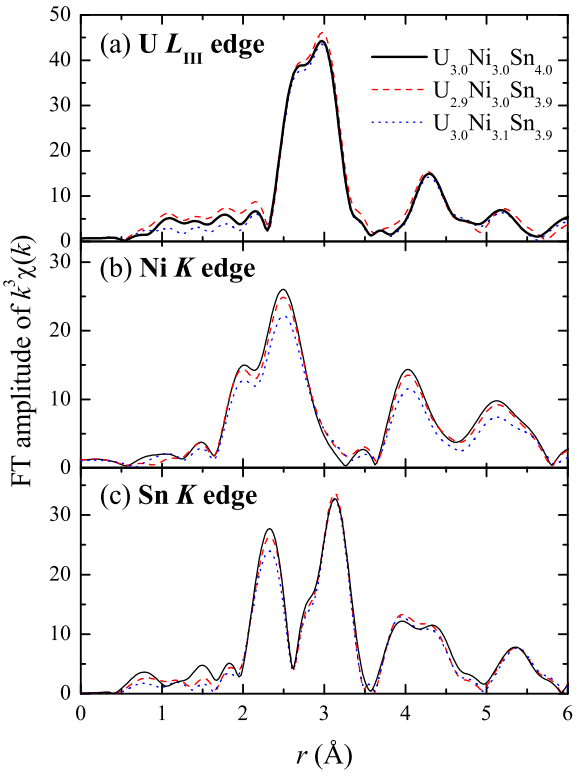

FIG. 4: Fourier transforms of the $k^3\chi(k)$ XAFS data for the powder samples. U and Sn (transmission) transforms are from k=3.0-15 Å^{-1}, while the Ni (fluorescence) transform is from 2.5-12.0 Å^{-1}, all Gaussian narrowed by 0.3 Å^{-1}.

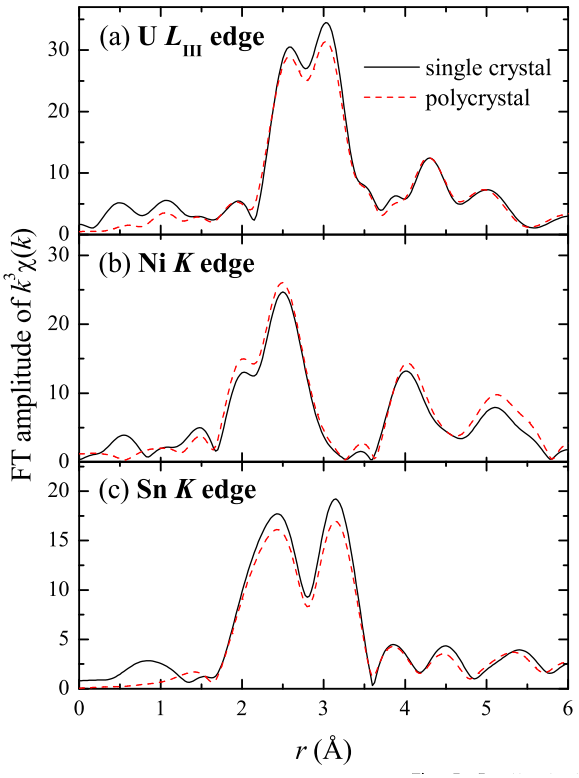

FIG. 5: Fourier transforms of the $k^3\chi(k)$ XAFS data comparing the polycrystal and the single crystal data for the nominally $U_3Ni_3Sn_4$ samples with consistent transform ranges. U and Sn transforms are from k=3.0-13 Å^{-1} while the Ni transform is from 2.5-12.0 Å^{-1}, all Gaussian narrowed by 0.3 Å^{-1}.

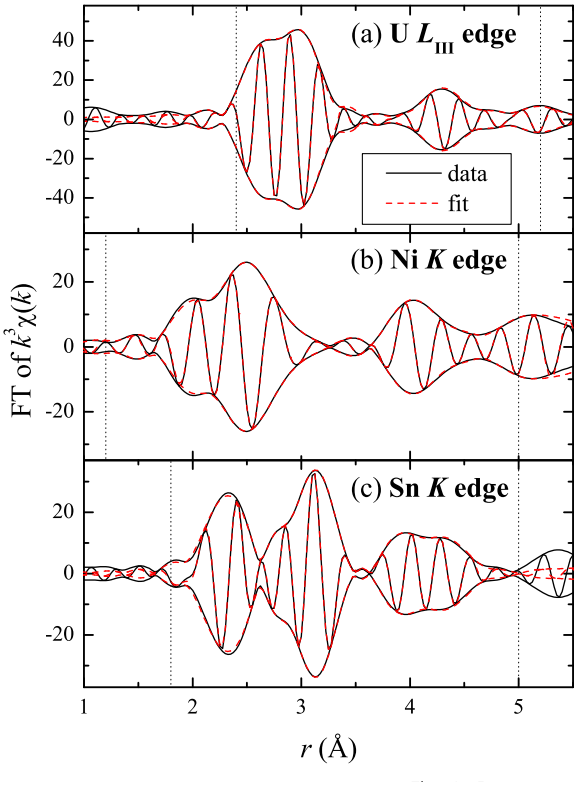

FIG. 6: Examples of the fits to the (a) U $L_{\rm III}$ and the (b) Sn K polycrystal data. Each transform is represented by three lines. The inner oscillating line is the real part of the complex transform, while the envelope lines are $\pm$ the amplitude of the transform. Vertical dotted lines show the r-space fit range. Transform ranges are as in Fig. 4.

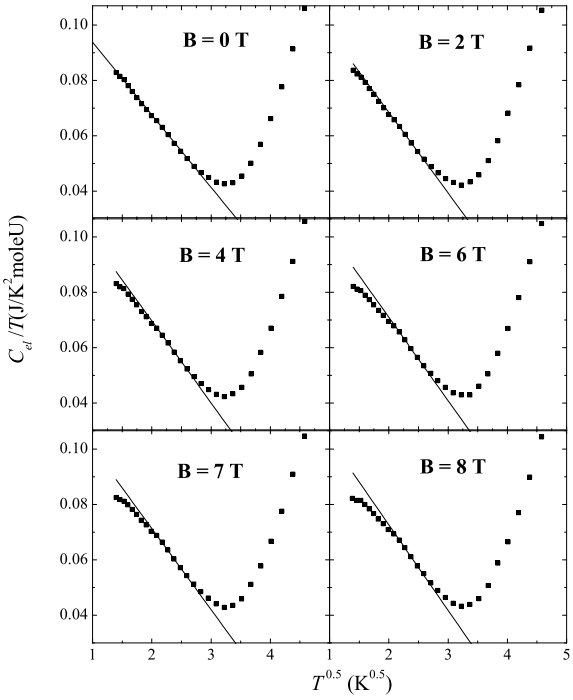

FIG. 7: C_{el}/T as a function of $T^{0.5}$ of $U_3Ni_3Sn_4$ single crystal for B = 0, 2, 4, 6, 7, 8 T. The straight line is a guide to the eye for the $C_{el}/T \sim T^{0.5}$ behavior.

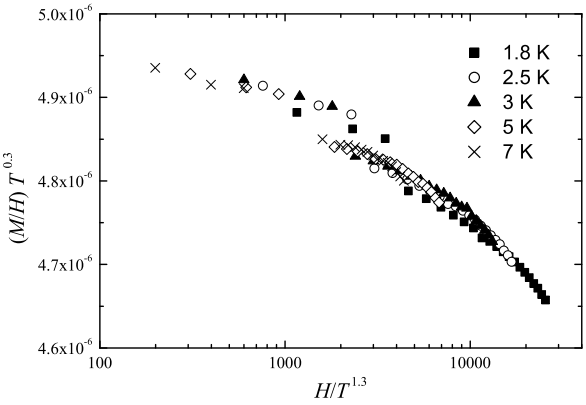

FIG. 8: The magnetization of $U_3Ni_3Sn_4$ as a function of applied field H and temperature. Data are plotted as $(M/H)T^{0.3}$ vs. $\log(H/T^{1.3}$ to reveal scaling exponent.

Tables

TABLE I: Final fit parameters to the U $L_{\rm III}$, Ni K and Sn K edge data at 20 K on three polycrystal samples of $U_3Ni_3Sn_4$ with various nominal stoichiometries. U $L_{\rm III}$ edge fits have $S_0^2 = 0.73 \pm 0.06$ and $\Delta E_0 = -10.3 \pm 0.4$. Ni K edge fits are from 2.5 to 13.0 Å^{-1} (Gausian narrowed by 0.3 Å^{-1}) and from 1.4 to 5.0 Å, and have $S_0^2 = 0.64 \pm 0.04$ and $\Delta E_0 = -0.5 \pm 0.5$. Sn K edge fits have $S_0^2 = 0.95 \pm 0.06$ and $\Delta E_0 = -8.3 \pm 0.1$. Diffraction data is provided for comparison ($R_{\rm diff}$) and is from Ref. 20 on a single crystal sample of $U_3Ni_3Sn_4$ collected at room temperature.

			$U_3Ni_3Sn_4$				$U_{2.9}Ni_{3.0}Sn_{3.9}$				$U_{3.0}Ni_{3.1}Sn_{3.9}$			
pair	N	$R_{\rm diff}$	R	σ^2	$\sigma^2_{\rm static}$	$\Theta_{\rm cD}$	R	σ^2	$\sigma^2_{\rm static}$	$\Theta_{\rm cD}$	R	σ^2	$\sigma^2_{\rm static}$	$\Theta_{\rm cD}$
U-Ni	4	2.864	2.848(3)	0.0018(2)	-0.0009(4)	252(5)	2.848(4)	0.0019(4)	-0.0004(5)	282(2)	2.848(3)	0.0019(2)	-0.0005(5)	259(4)
U-Sn	8	3.237	3.228(2)	0.0011(2)	-0.0006(3)	241(1)	3.226(4)	0.0009(2)	-0.0009(3)	231(1)	3.226(3)	0.0009(2)	-0.0007(3)	233(1)
U-U	8	4.374	4.36(1)	0.0016(3)	-0.0005(3)	164(6)	4.355(5)	0.0014(2)	-0.0005(3)	173(2)	4.355(3)	0.0014(2)	-0.0000(3)	169(3)
U-Ni	2	4.676	4.67(1)	0.0015(3)			4.67(1)	0.0022(6)			4.67(1)	0.0022(4)		
Sn-Ni	3	2.609	2.604(3)	0.003(1)	0.001(1)	420(15)	2.597(3)	0.0027(2)	-0.0003(2)	349(4)	2.599(3)	0.0027(2)	0.0008(3)	359(3)
Sn-U	6	3.237	3.223(5)	0.0006(4)	-0.0017(5)	202(12)	3.232(7)	0.0016(2)	-0.0004(2)	246(2)	3.228(3)	0.0012(2)	-0.0004(2)	273(5)
Sn-Sn	3	3.497	3.50(3)	0.003(3)	-0.003(3)	172(17)	3.500(4)	0.004(1)	-0.000(1)	245(6)	3.496(3)	0.0017(5)	-0.0001(6)	250(20)
Sn-Sn	2	4.050	3.98(3)	0.003(3)			4.03(1)	0.01(1)			4.02(1)	0.0024(7)		
Sn-Ni	3	4.232	4.25(3)	0.002(1)			4.16(5)	0.01(1)			4.22(1)	0.005(2)		
Sn-Sn	6	4.594	4.60(3)	0.002(1)			4.598(4)	0.0034(3)			4.596(3)	0.0023(2)		
Ni-Sn	3	2.609	2.588(4)	0.0017(4)	-0.0004(5)	347(10)	2.585(6)	0.0014(3)	-0.0007(3)	334(10)	2.587(4)	0.0017(6)	0.0003(6)	353(4)
Ni-U	3	2.864	2.850(6)	0.0028(6)	0.0003(7)	252(7)	2.850(8)	0.0023(5)	-0.0005(5)	234(7)	2.853(6)	0.002(1)	-0.0005(9)	234(4)
Ni-Sn	3	4.231	4.24(1)	0.0005(9)			4.26(1)	0.000(2)			4.25(2)	0.004(3)		
Ni-Ni	3	4.374	4.35(1)	0.001(1)			4.35(1)	0.000(1)			4.37(1)	0.001(2)		
Ni-U	3	4.676	4.70(5)	0.005(7)			4.70(3)	0.003(4)			4.70(3)	0.003(2)		